Journal of Engineering and Sustainable Development
Vol. 29, No. 06, November 2025
https://jeasd.uomustansiriyah.edu.iq/index.php/jeasd
ISSN 2520-0917
Research Article
https://doi.org/10.31272/jeasd.2630

First and Second-Order Sliding Mode Control Strategy of Buck-Boost Converter for Photovoltaic System

Jannat M. Saied*, Riyadh G. Omar

Electrical Engineering Department, College of Engineering, Mustansiriyah University, Baghdad, Iraq.

*Email: Jannat.M@uomustansiriyah.edu.iq

Article Info

Received 28/04/2024
Revised 02/09/2025
Accepted 15/09/2025

Abstract

This study presents the modeling and simulation of a Buck-Boost converter designed for photovoltaic applications. The converter is controlled by a sliding mode control (SMC) technique, which has several advantages when utilized in DC-DC power converters. The design was simulated using MATLAB R2023a. To obtain more realistic results, the study used local solar irradiation during the summer months as the radiation incident on solar panels. The battery maintains voltage stability even during periods without solar irradiation. The results emphasized the advantages of the control method for producing a stable, long-lasting output voltage despite fluctuations in solar irradiation and uncertainty in system parameter values. Additionally, the control method reduces the tracking error to zero and speeds up the connection to the reference voltage. This work employs a second-order sliding-mode control strategy, specifically the super-twisting algorithm, to mitigate the chattering phenomenon commonly associated with first-order sliding mode. The effectiveness of the second-order sliding mode control (SOSMC) was confirmed by Fast Fourier Transform (FFT) analysis, which revealed a 75% reduction in total harmonic distortion (THD).

Keywords: Chattering effect, Higher order sliding mode control, Sliding mode control, Super-twisting algorithm

1. Introduction

Using fossil fuels, such as coal, natural gas, and oil, significantly contributes to atmospheric pollution and environmental degradation worldwide. Global energy investments are increasingly shifting towards sustainable energy sources, with renewable energy pivotal in producing clean energy [1], [2]. Photovoltaic power is a renewable energy source that has gained popularity due to the rapid growth of power electronics technology [3]-[5]. Solar power is widely used globally due to its clean, noiseless nature. The unique characteristics of photovoltaic technology make it the ultimate example of a highly sought-after renewable energy source [6].

Regrettably, photovoltaic systems face two primary obstacles: their conversion efficiency is subpar, and the electricity generated by solar panels fluctuates significantly with weather conditions. Moreover, the produced power out of any PV (photovoltaic) system depends on various elements, including solar energy, air temperature, and the properties of the connected load, as a result of the nonlinear behavior of their power-voltage (P-V) and current-voltage (I-V) characteristics. To optimize solar cell utilization, it is essential to use MPPT (maximum power point tracking). Integrating such trackers can reduce the cost of electricity generated by solar panels [7].

Performance metrics, including precision, dynamic behavior, and intricacy, can be used to assess different approaches to achieving optimal power extraction. Nevertheless, it is frequently more advantageous to classify MPPT algorithms into four distinct types: conventional, intelligent, optimization, and hybrid [8].

Among the MPPT command options, Perturb & Observe (P&O) is notable for its widespread use. This is due to its uncomplicated structure and the diminished number of parameters. The main idea is to alter the duty ratio D in either an upward or downward direction, create disturbances, and then assess the impact on the PV panel's output power. It is essential to highlight that the disturbance ΔV is kept at a minimum to avoid excessive swings in power [9].

According to the prevailing academic literature, converters in the direct current (DC) field are often regarded as the crucial element within all hybrid renewable energy systems. DC-DC converters regulate a specific output voltage, which may be affected by intermittent conditions and imperfections in circuit components and switches [10].

Control engineers face significant challenges in controlling DC-DC converters. Many industries use linear controllers, such as PI or PID controllers, to control converters due to their cost-effectiveness and simplicity. However, these controllers must improve their flexibility when faced with parameter changes, such as major fluctuations in load or input voltage. The control strategy for DC-DC converters must account for the fact that they are nonlinear systems that experience changes in load and input voltage. They must also ensure stability under all operating conditions. Therefore, researchers have focused on robust and flexible nonlinear controllers to optimize the performance of DC-DC converters. Sliding mode controllers (SMCs) are widely recognized for their stable performance and flexible control [11].

Tong et al. [12] propose the use of a slide-mode controller to enhance the performance of a DC-DC boost converter for PV applications. The system has two control loops: a current loop for calculating the duty cycle of the frequency switch, and an input-voltage loop guided by the MPPT algorithm to determine the inductor current. The results show reduced steady-state error, settling time, and overshoot compared to slide-mode plus proportional integration (SMPI) controllers.

Walid et al. [13] propose a third-order sliding modulus control (TOSMC) scheme to determine the MPP of a PV system under various weather conditions. The components of the system are a DC-DC boost converter, a PV panel, a load, and an MPPT technique. Simulations performed in MATLAB demonstrate reduced steady-state error and improved overall efficiency.

Kayisli [14] investigates the use of solar energy as a sustainable energy option, with a specific emphasis on MPPT control via sliding-mode control. Chattering issues are mitigated by designing a super-twisting sliding mode controller (STSMC) with a type-2 fuzzy set.

Kaplan and Bodur [15] introduce a transformer-less DC-DC power boost converter that employs a switched-capacitor architecture and a sliding-mode controller to increase the output voltage of PV panels for grid applications. The investigation involves a mathematical and practical examination of voltage and currents, utilizing a 300 W installed hardware.

RakhtAla et al. [16] introduce a new SMC for a DC-DC converter to regulate the output voltage. MATLAB/Simulink simulations were conducted to evaluate the controller with different DC–DC converters. The controller can provide stability and robustness under uncertainty, load variations, and changes in input voltage.

Inomoto et al. [17] present a novel approach to optimize the controllers of boost converters in PV systems. The Genetic Algorithm (GA) is utilized to optimize SMC and SMPIC (Sliding Mode Plus Proportional-Integrative). The experimental results are assessed using hardware, providing evidence of reduced overshoot and settling time.

Alam et al. [18] provide a novel hybrid controller for DC-DC boost converters that integrates a backstepping controller and a nonsingular fast terminal sliding mode controller (NFTSMC). The controller's resilience and efficacy are verified under a variety of input voltage, reference voltage, and power demand fluctuations.

The article by Waghmare and Chaturvedi [19] details the methodology for controlling high-order sliding mode (HOSM) in SPV-isolated flyback converters. This approach surpasses traditional PI control techniques in the face of uncertainty. Furthermore, it introduces a unique method for preventing chattering in flyback converters by employing STSMC.

This study aims to design and evaluate a robust Buck-Boost converter controlled by first- and second-order sliding mode control (SMC and SOSMC) for PV systems under fluctuating solar irradiance in Baghdad. The proposed work introduces a new design that differs from previous works. The design incorporates a DC-to-DC Boost converter, with its switch signal controlled by an MPPT to track the MPP when solar irradiance fluctuates. The Boost converter charges a battery, with bidirectional control managing its energizing and depleting the charge. The purpose of the battery is to maintain a steady voltage regardless of weather, charging when solar irradiance is available and discharging when it's not. The battery connects to a Buck-Boost converter, controlled by SMC, to provide a consistent output voltage that is resilient to system parameter changes and solar irradiation fluctuations. To address SMC's chatter issue, second-order sliding mode control (SOSMC), specifically the super-twisting algorithm (STSMC), was employed. The effectiveness of the proposed design was tested through MATLAB simulations, using local solar irradiation data from Baghdad during the summer to achieve more realistic results.

2. Method of the Research

The methodology of this study involves four main stages. First, a mathematical model of the Buck–Boost DC-DC converter was derived using state-space representation, defining the relationships among current, voltage, and control variables. Second, two control strategies—first-order Sliding Mode Control (SMC) and Second-Order Sliding Mode Control (SOSMC) based on the super-twisting algorithm—were designed to enhance system robustness and mitigate chattering. Third, the proposed control schemes were implemented and simulated in MATLAB/Simulink (R2023a) using locally measured solar irradiation data from Baghdad during summer to ensure realistic environmental conditions. Finally, the system's dynamic response, voltage tracking performance, and harmonic distortion were analyzed and compared under varying solar irradiance and load resistance.

2.1. Buck-boost DC-DC converter paradigm

A Buck-Boost converter controls an output voltage that can be set to be greater or less than the input voltage. The polarity of the output voltage is distinct from that of the input voltage. The converter topology is depicted in Fig. 1 [16].

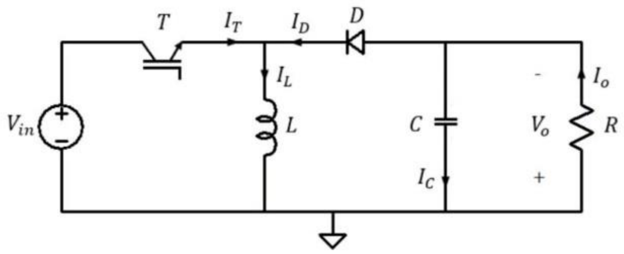

Figure 1. Buck-Boost converter circuit model.

The state-space form of the converter is derived by applying the fundamental laws governing the system's operation. The circuit is modified to derive the state equations incorporating the converter's control input (u). The control input u represents the switch position.

When the switch (T) is on for a time (DT): u=1

$$\frac{di_L}{dt} = \frac{1}{L} v_{boost} \quad (1)$$

$$\frac{dv_c}{dt} = -\frac{1}{Rc} v_c \quad (2)$$

When the switch (T) is off for a time (1-D) T: u=0

$$\frac{di_L}{dt} = \frac{1}{L} v_c \quad (3)$$

$$\frac{dv_c}{dt} = -\frac{1}{c} i_L - \frac{1}{RC} v_c \quad (4)$$

The converter state equations can be obtained by combining these two sets of equations with the control input u.

$$\dot{x}_1 = \frac{1-u}{L} x_2 + \frac{u}{L} v_{boost} \quad (5)$$

$$\dot{x}_2 = -\frac{1-u}{c} x_1 - \frac{1}{Rc} x_2 \quad (6)$$

Where:

T = Ideal IGBT switch

DT = The duration during which the switch is closed

T(1-D) The duration during which the switch is open

To derive a state-space model of the form $x^{\cdot} = Ax(t) + Bu(t)$, the dynamics of the system can be mathematically expressed as:

$$x_1 = I_L \ , x_2 = v_c$$

$$\dot{x}_1 = \frac{1}{L} x_2 + \frac{u}{L}(v_{boost} - x_2) \quad (7)$$

$$\dot{x}_2 = -\frac{1}{c} x_1 - \frac{1}{RC} x_2 + \frac{u}{c} x_1 \quad (8)$$

2.2. Sliding mode control (SMC)

This study focuses on a robust control strategy that drives the system's trajectory toward a predefined surface, where a switching rule regulates the system's behavior. The aim is to develop a switching law and sliding surface to effectively achieve the specified control objectives, encompassing stability, precise tracking, and rejection of disturbances [12].

2.2.1. First-order sliding mode control

- **Sliding surface**

The sliding function in a standard sliding mode control approach is determined by the error, its derivative, or its second derivative, and can be extended. The objective is to incorporate all variables into the sliding line, set them to zero, and rely only on the error and a designated coefficient, without depending on the system's parameters [20].

$$s = (x_2 - v_{ref}) + B(x_1 - I_{Lref}) \quad (9)$$

Where:

v_{ref} = The reference voltage defines the desired value of the converter's output voltage.

I_{Lref} = The reference current specifies the desired value of the inductor current in the converter.

B The sliding coefficient is adjusted to attain the required performance.

- **Parameter uncertainty in the model of the Buck-Boost converter**

$$\frac{1}{L} = \frac{1}{L_{nom}} + \Delta_L \quad (10)$$

$$\frac{1}{R} = \frac{1}{R_{nom}} + \Delta_R \quad (11)$$

$$\frac{1}{c} = \frac{1}{c_{nom}} + \Delta_c \quad (12)$$

Where:

$\frac{1}{L_{nom}}, \frac{1}{R_{nom}}, \frac{1}{c_{nom}}$ are the nominal values

Δ_L, Δ_R, and Δ_c are bounded disturbances

- **Determination of control signal (U)**

The overall control structure, denoted as u, comprises two distinct components: a nonlinear element and an equivalent control element.

A nonlinear element aids in bringing all of the variables from their initial states toward the target surface and keeps them close to the desired trajectory.

An equivalent control element: It reduces the time delay during the reaching phase; it may occasionally introduce complexity to the control input.

$$u = u_{eq} + u_n \quad (13)$$

$$\dot{s} = \dot{x}_2 + B\dot{x}_1 \quad (14)$$

Where:

u_n Nonlinear element

u_{eq} Equivalent control element

(15) is obtained by substituting (7) and (8) into (14) and equating the derivative of S with zero.

$$-\frac{1}{c}x_1-\frac{1}{RC}x_2+\frac{u}{c}x_1+B\left[\frac{1}{L}x_2+\frac{u}{L}(v_{boost}-x_2)\right]=0 \quad (15)$$

By solving (15), the value of u_{eq} was obtained.

$$u_{eq}=\frac{\frac{1}{C}x_1+\frac{1}{RC}x_2-\frac{B}{L}x_2}{\frac{1}{C}x_1+\frac{B}{L}(v_{boost}-x_2)} \quad (16)$$

$$u_n=-u_0\,sgn\big(s(x)\big) \quad (17)$$

$$sgn\big(s(x)\big)=\begin{cases}1 & s>0\\ 0 & s=0\\ -1 & s<0\end{cases} \quad (18)$$

- **Stability analysis**

The control approach aims to compel the system states to converge onto the designated surface from any beginning condition and maintain them there. This requirement is satisfied by the Lyapunov function, a mathematical tool used to analyze the stability of a dynamical system. The Lyapunov function (V) is defined as follows:

$$V=\frac{1}{2}S^2 \quad (19)$$

To guarantee the stability of the controller and the convergence of the state trajectory to the designated surface, the proposed switching control law must satisfy the Lyapunov stability condition, i.e., the time derivative of the Lyapunov function V must remain strictly negative [20]. In other words, the following inequality needs to be met:

$$\dot{V}=s\dot{s}<0 \quad (20)$$

$$\dot{s}=-\Delta_c x_1-\left(\Delta_R\frac{1}{c_{n^0m}}+\frac{1}{R_{n_0m}}\Delta_c+\Delta_c\Delta_R\right)x_2+\Delta_C x_1 u_n+B[\Delta_L x_2+\Delta_L(v_{boost}-x_2)u_n] \quad (21)$$

$$u_0>\left|\frac{\left[\Delta c x_1+\left(\frac{1}{c_{nom}}\Delta_R+\frac{1}{R_{nom}}\Delta c+\Delta_R\Delta_C-B\Delta_L\right)x_2\right]}{B\Delta_L(v_{boost}-x_2)+\Delta_C x_1}\right| \quad (22)$$

- **Determination of I_{Lref}**

$$I_{L_r}=\frac{v_{ref}}{R}\left(\frac{v_{ref}}{v_{boost}}-1\right) \quad (23)$$

2.2.2. Second-Order Sliding Mode Control

This type of variable-structure control offers several advantages, including reduced-order compensated dynamics, finite-time convergence, and robustness. This method uses high-frequency switching to drive the variables to zero. However, there are cases where such switching is impractical, and continuous control becomes necessary. To address this issue, a continuous control technique known as "super twisting" ensures finite-time convergence. The sliding surface and equivalent control element are chosen to be the same as in first-order SMC. The calculation of second-order sliding mode control involves computing an additional derivative of the sliding surface. The representation of the controlled system can be stated as:

$$\ddot{s}=\phi(x,t)+\gamma(x,t)\dot{u} \quad (24)$$

By replacing (7) and (8) with their respective values in (21) and subsequently rearranging the equations

$$\ddot{s}=-\frac{1}{c}\left[\frac{x_2}{L}+\frac{u}{L}(v_{boost}-x_2)\right]+\left[\frac{B}{L}-\frac{1}{RC}\right]\left[-\frac{1}{c}x_2-\frac{1}{Rc}x_2+\frac{u}{c}x_2\right]+\left[\frac{1}{c},\frac{x_2}{L}+\frac{u}{L}(v_{boost}-x_2)-\frac{B}{L}\left(-\frac{1}{c}x_1-\frac{1}{Rc}x_2+\frac{1}{c}x_1 u\right)\right]u+\left[\frac{1}{C}x_1+\frac{B}{L}(v_{boost}-x_2)\right]\dot{u} \quad (25)$$

$$u_n=u_{n_1}+u_{n_2} \quad (26)$$

$$\dot{u}_{n_1}=-M\,sgn(s) \quad (27)$$

$$u_{n_2}=-\lambda|s|^{0.5}\,sgn(s) \quad (28)$$

$$u_n=-\lambda|s|^{0.5}\,sgn(s)-M\int sgn(s)\,dt \quad (29)$$

Where: λ, M Positive design constants. The necessary conditions for guaranteeing finite-time convergence of the system to the sliding manifold are as follows:

$$-\psi<\emptyset<\psi \quad (30)$$

$$\Gamma_m<\gamma<\Gamma_M \quad (31)$$

$$M>\frac{\psi}{\Gamma_m} \quad (32)$$

$$\lambda^2\geq\frac{4\psi\Gamma_m(M+\psi)}{\Gamma_m^2\Gamma_m(M-\psi)} \quad (33)$$

The super-twisting control remains continuous due to the continuity of both $\mathbf{u_{n_1}}$ and the term $\mathbf{u_{n_2}}$. The term sgn(s) of high-frequency switching is concealed within the integral.

3. Simulation and Results

To verify the theoretical analysis presented in this paper, MATLAB R2023a software is employed to simulate the proposed design. The overall design is depicted in Fig. 2; in this model, a PV array comprising 22 panels in parallel and 17 in series is used to generate 100 kilowatts of power. Details about the panels are in Table 1.

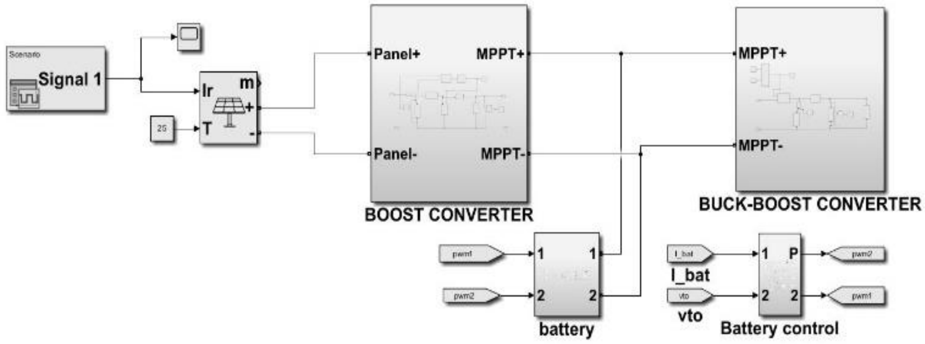

Figure 2. Buck-boost converter circuit model.

Table 1. PV array parameters.

Data	Value
open circuit voltage (Voc)	39.2 Volt
short circuit current (Ish)	9.44 Amper
voltage at MPP (Vmpp)	30.9 Volt
current at MPP (Impp)	8.81 Amper
Vpenal	17(panels) * 30.9 = 525.3 V
Ipanel	22(panels) * 8.81 = 193.8 A
Ppanel	525.3 * 193.8 = 101.8 KW

One of the subsystems is the boost converter, which is controlled using MPPT. Specifically, the P&O is employed to track the MPP of the solar panel, accounting for changes in solar irradiation. Fig. 3 provides a visual of this subsystem. The study utilizes local solar irradiation data from the city of Baghdad during the summer months.

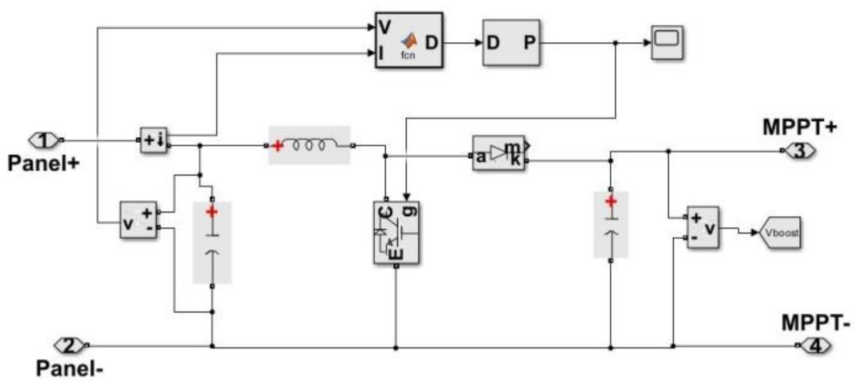

Figure 3. Overall boost converter subsystem.

Furthermore, an MPP controller is used to increase the array voltage, which is necessary to charge the battery. Table 2 provides more information about the battery. A 1000 V voltage level is achieved by connecting the battery to a Buck-Boost converter controlled using two different techniques.

Table 2. Battery parameters.

Data	Value
Rated capacity	100 Ah
Initial state of charge	100 %
Battery response time	30 sec
Nominal voltage	500 V

Fig. 4 depicts this subsystem. Table 3 provides more details on the converter parameters. Fig. 5 illustrates the MATLAB representations of equations 9, 10, 13, 14, and 19. Fig. 6 shows the modeling of Equation 26. Constants used in second-order SMC M=20, $\lambda = 0.01$.

Table 3. Parameters of boost & Buck-Boost converters.

	MPPT MODEL on boost converter	SMC MODEL on Buck-Boost converter
Capacitance	10 mF	1 mF
Inductance	33 mH	400 mH
Input voltage	525.3 V	651 V
B	-	1000
Switching frequency (Fsw)	-	4KHZ

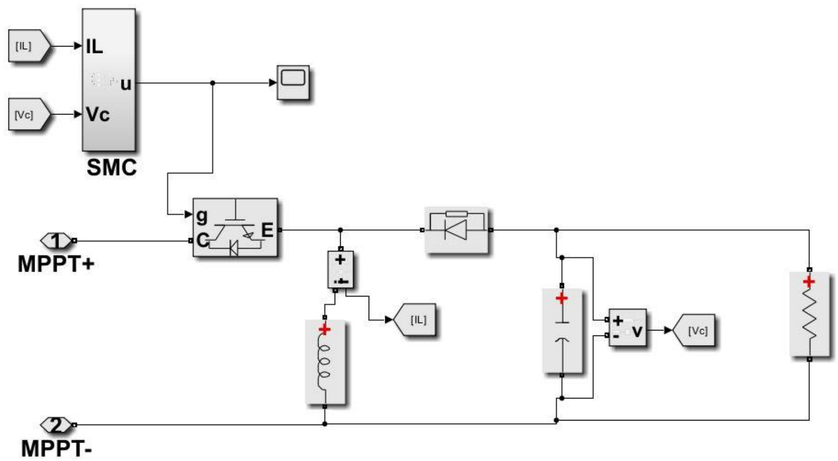

Figure 4. A subsystem of a Buck-Boost converter.

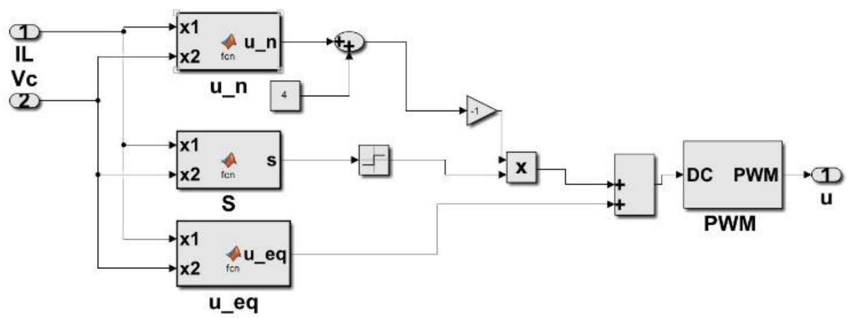

Figure 5. Block diagram of first-order sliding mode control.

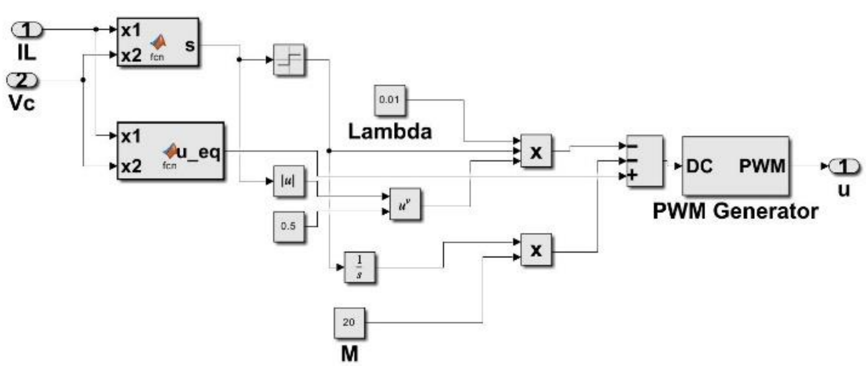

Figure 6. Block diagram illustrating the second-order sliding mode control.

Fig. 7 depicts the Buck–Boost converter output voltage utilizing first-order sliding mode control. The graph uses green to depict the fluctuating local solar irradiance throughout the day. The irradiation begins at 0 W/m2 and increases gradually to 370.5 W/m2 by 7:00 am. By 12:00 pm, it reaches 938.5 W/m2 and remains constant thereafter. The irradiance drops to 781.8 W/m2 at 2:00 pm and further reduces to 435 W/m2 at 4:00 pm.

The reduction persists until 7:00 pm, after which the irradiation remains at zero for the remainder of the day. The red color in the figure represents the Buck–Boost converter output voltage, while the blue color represents the reference voltage.

Fluctuations in irradiation levels can have a major impact on the panel voltage, leading to a drastic drop. Despite the fluctuations, the control unit demonstrated a rapid and reliable response. The presence of the battery ensures a stable output voltage. It operates in a charging state when solar irradiation is available. When solar irradiation is absent, the solar panels do not produce power, and the battery discharges to provide the converter with input voltage.

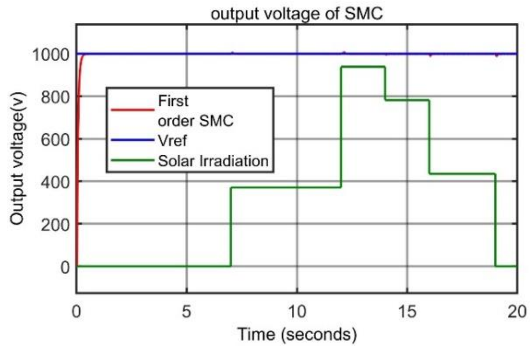

Figure 7. Buck-Boost converter output voltage under local irradiation (first-order).

Fig. 8 and 9 depict the converter's output voltage as the resistive load changes, along with the corresponding sliding coefficient, which achieves the required controller performance.

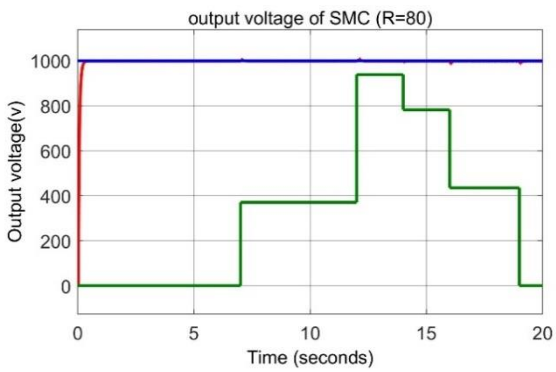

Figure 8. Buck-Boost converter output voltage at R= 80-ohm, B = 240.

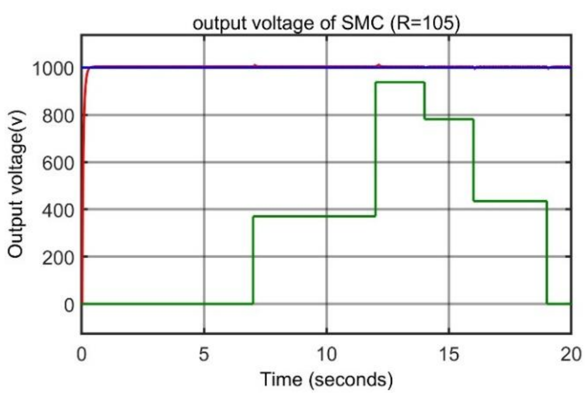

Figure 9. Buck-Boost converter output voltage at R = 105-ohm, B = 2010.

Fig. 10 shows the Buck-Boost converter output voltage while implementing second-order sliding mode control.

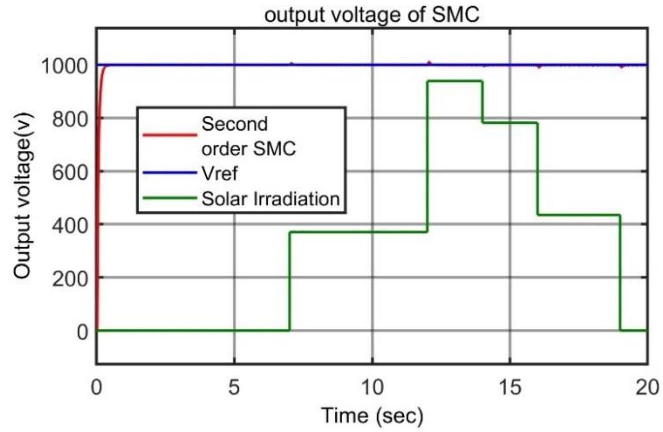

Figure 10. Buck-Boost converter output voltage under local irradiation (second-order).

To demonstrate the efficacy of the suggested SOSMC control mechanism in mitigating chatter. The converter's output voltage signal was examined using a fast Fourier transform (FFT) with first- and second-order SMC techniques. The results demonstrated that SOSMC effectively reduced total harmonic distortion (THD%) from 0.04% to 0.01%. This reflects a decrease in noise impact and an improvement in energy conversion efficiency. Fig. 11 and 12 display the FFT analysis results for the output voltage signals of the first- and second-order SMC implementations, respectively.

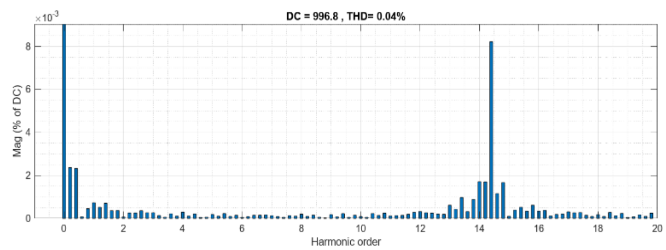

Figure 11. FFT analysis of first-order SMC output voltage.

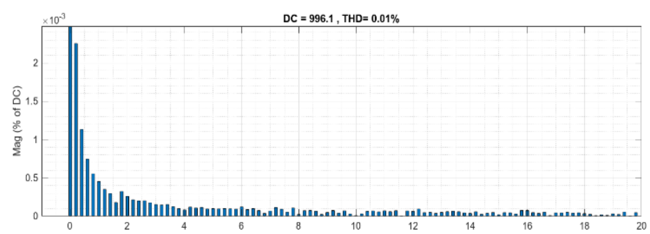

Figure 12. FFT analysis of second-order SMC output voltage.

The results of the solar panels are shown in Fig. 13, which displays the voltage, current, and output power. As mentioned before, the panels' output is highly influenced by fluctuations in solar radiation. Every sudden change in irradiation causes a significant drop in values, which is referred to as the transient state. The figure below (right) shows the output voltage of a boost converter, which is the voltage required to charge the battery.

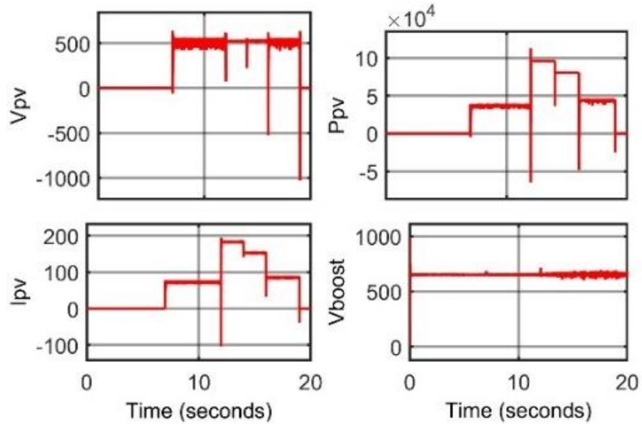

Figure 13. The results of solar panels.

Lastly, Fig. 14 presents the battery results, including voltage, current, and state of charge (SOC). The battery discharges during the 0-7 sec period when solar irradiation is absent and charges during periods of solar irradiation.

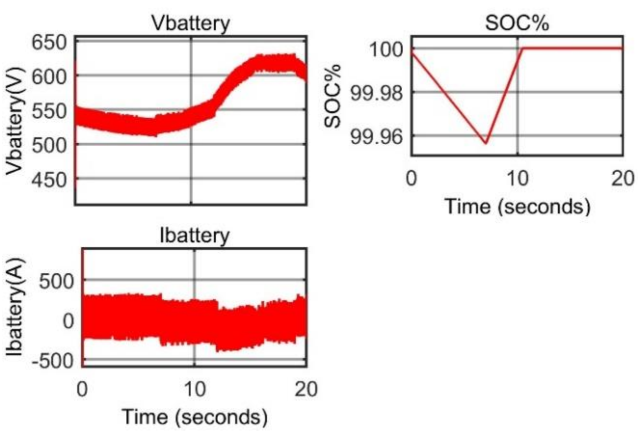

Figure 14. The results of the battery.

4. Conclusions

A control strategy for the Buck-Boost converter was developed, incorporating both first- and second-order variable-structure techniques. The results demonstrated that this approach effectively achieved the required reference voltage quickly and reduced the tracking error to zero. The study also highlighted the advantages of the control method in maintaining the stability of the output voltage relative to the reference voltage, even when solar radiation, input voltage, and system parameter uncertainties vary. Additionally, the study discussed the significance of the slip coefficient in attaining the desired performance through the application of variable load resistance. To address SMC's chatter issue, SOSMC was employed, specifically the STSMC. The second-order SMC design reduced chattering, as evidenced by a 75 percent decrease in total harmonic distortion.

One of the main challenges the authors face is the need to use a trial-and-error approach to determine the gain values for the proposed control methods. This method is computationally intensive and does not ensure optimal gains. In future work, the researchers recommend using modern optimization techniques such as fuzzy logic, particle swarm optimization, and others. These techniques reduce the time and effort required for the task and ensure the best possible gains.

Acknowledgments

The authors wish to express gratitude to Mustansiriyah University College of Engineering for their support and encouragement.

Conflict of interest

The authors declare that there are no conflicts of interest regarding the publication of this manuscript.

Author Contribution Statement

Jannat M. Saied and Riyadh G. Omar collaborated on a research project that investigated a specific problem in their field of study. Jannat M. Saied developed the theoretical framework, performed the computational analysis, and generated the initial findings. Both authors verified the analytical methods used in the study, investigated a specific aspect of the problem, and supervised the project's overall progress. The authors collaborated in analyzing the results and contributed to the final manuscript.

References

[1] M. Majid Gulzar, H. Tehreem, and M. Khalid, "Modified Finite Time Sliding Mode Controller for Automatic Voltage Regulation under Fast-Changing Atmospheric Conditions in Grid-Connected Solar Energy Systems," *International Journal of Intelligent Systems*, vol. 2023, p. 8863346, 2023. https://doi.org/10.1155/2023/8863346

[2] R. A. Mejeed, "Resilient Photovoltaic-Battery Systems for Urban Households in Grid-Interrupted Environments: a Baghdad Case Study," *Energy Storage*, vol. 7, no. 7, Sep. 2025, doi: https://doi.org/10.1002/est2.70264

[3] R. Marouani, K. Echaieb, and A. Mami, "Sliding mode controller for buck-boost DC-DC converter in PV grid-connected system," in *2012 16th IEEE Mediterranean Electrotechnical Conference*, 2012, pp. 281-284. https://doi.org/10.1109/melcon.2012.6196433

[4] S. Amirreza Abdollahi, S. Faramarz Ranjbar, and M. Jafari, "Numerical investigation of increasing the efficiency of thermal photovoltaic system by changing the level of heat transfer distribution," *Case Studies in Thermal Engineering*, vol. 54, p. 103989, 2024/02/01/ 2024. https://doi.org/10.1016/j.csite.2024.103989.

[5] B. Basantes, F. Ulloa-Herrera, M. Pozo, and O. Camacho, "Power management of an off-grid photovoltaic system using a linear algebra-based control," *Results in Engineering*, vol. 23, p. 102375, 2024/09/01/ 2024. https://doi.org/10.1016/j.rineng.2024.102375.

[6] A. Chouder, S. Silvestre, N. Sadaoui, and L. Rahmani, "Modeling and simulation of a grid connected PV system based on the evaluation of main PV module parameters," *Simulation Modelling Practice and Theory*, vol. 20, pp. 46-58, 2012. https://doi.org/10.1016/j.simpat.2011.08.011

[7] L. Hernández-Callejo, S. Gallardo-Saavedra, and V. Alonso-Gómez, "A review of photovoltaic systems: Design, operation and maintenance," *Solar Energy*, vol. 188, pp. 426-440, 2019. https://doi.org/10.1016/j.solener.2019.06.017

[8] C. B. Oguz, E. Avci, and S. B. Ozturk, "Analysis of PV power plant performance considering combination of different MPPT algorithms, shading patterns, and connection types," *Engineering Science and Technology, an International Journal*, vol. 48, p. 101559, 2023. https://doi.org/10.1016/j.jestch.2023.101559

[9] M. Ourahou, W. Ayrir, and A. Haddi, “Current correction and fuzzy logic optimizations of Perturb & Observe MPPT technique in photovoltaic panel,” *International Journal for Simulation and Multidisciplinary Design Optimization*, vol. 10, p. A6, 2019, doi: https://doi.org/10.1051/smdo/2019007

[10] S. Huerta-Moro, O. Martínez-Fuentes, V. R. Gonzalez-Diaz, and E. Tlelo-Cuautle, “On the Sliding Mode Control Applied to a DC-DC Buck Converter,” *Technologies*, vol. 11, no. 2, pp. 33–33, Feb. 2023, doi: https://doi.org/10.3390/technologies11020033

[11] J. Zhang, D. G. Dorrell, L. Li, and A. Argha, "A novel sliding mode controller for DC-DC boost converters under input/load variations," in *IECON 2015-41st Annual Conference of the IEEE Industrial Electronics Society*, 2015, pp. 001698-001703. https://doi.org/10.1007/s40313-018-00427-w

[12] D. Tong, C. Xu, Q. Chen, and W. Zhou, "Sliding mode control of a class of nonlinear systems," *Journal of the Franklin Institute,* vol. 357, no.3, pp. 1560-1581, 2020. https://doi.org/10.1016/j.jfranklin.2019.11.004

[13] K. Walid, M. Sofiane, H. Benbouhenni, G. Hamza, and T. Es-saadi, "Application of third-order sliding mode controller to improve the maximum power point for the photovoltaic system," *Energy Reports,* vol. 9, pp. 5372-5383, 2023. https://doi.org/10.1016/j.egyr.2023.04.366

[14] K. Kayisli, "Super twisting sliding mode-type 2 fuzzy MPPT control of solar PV system with parameter optimization under variable irradiance conditions," *Ain Shams Engineering Journal*, vol. 14, no.1, p. 101950, 2023. https://doi.org/10.1016/j.asej.2022.101950

[15] O. Kaplan and F. Bodur, "Super Twisting Algorithm-Based Sliding Mode Controller for Buck Converter Feeding Constant Power Load," *International Journal of Renewable Energy Research,* vol. 12, no. 1, pp. 134-145, 2022. https://doi.org/10.20508/ijrer.v12i1.12448.g8383

[16] S. M. RakhtAla, M. Yasoubi, and H. HosseinNia, "Design of second-order sliding mode and sliding mode algorithms: a practical insight to DC-DC buck converter," *IEEE/CAA Journal of Automatica Sinica,* vol. 4, no. 3, pp. 483-497, 2017. https://doi.org/10.1109/jas.2017.7510550

[17] R. Inomoto, A. J. Sguarezi Filho, J. R. Monteiro, and E. C. M. da Costa, "Genetic algorithm-based tuning of sliding mode controllers for a boost converter of PV system using Internet of Things environment," *Results in Control and Optimization,* vol. 14, p. 100389, 2024. https://doi.org/10.1016/j.rico.2024.100389

[18] Z. Alam, S. K. Ghosh, A. F. Alkhateeb, T. K. Roy, M. S. Islam, S. Saha, *et al.*, "Robust hybrid nonlinear control approach for stability enhancement of a constant power load DC-DC boost converter," *Alexandria Engineering Journal,* vol. 74, pp. 535-545, 2023. https://doi.org/10.1016/j.aej.2023.05.041

[19] T. Waghmare and P. Chaturvedi, "A higher-order sliding mode controller’s super twisting technique for a DC–DC converter in photovoltaic applications," *Energy Reports,* vol. 9, pp. 581-589, 2023. https://doi.org/10.1016/j.egyr.2023.05.054

[20] M. Gursoy, *Sliding Mode Power Electronics Control for Stand-Alone Photovoltaic Energy Systems*: Southern Illinois University at Edwardsville, 2019.